Journal of Theoretical and Applied Information Technology
15th May 2023. Vol.101. No 9

ISSN: 1992-8645 www.jatit.org E-ISSN: 1817-3195

CNN-MOBILENETV2- DEEP LEARNING-BASED ALZHEIMER'S DISEASE PREDICTION AND CLASSIFICATION

AMBILI. A.V[1], DR. A.V. SENTHIL KUMAR, AND DR. ROHAYA LATIP[3]

[1] Research Scholar, PG Research and Computer Application, Hindusthan College of Arts and Science, Coimbatore.
[2]Director, PG and Research Department of Computer Applications, Hindusthan College of Arts & Science, Coimbatore
[3]Faculty of Computer Science and Information Technology, Universiti Putra Malaysia

E-mail: [1]ambili9009@gmail.com, [2]avsenthilkumar@yahoo.com, [3]rohayalt@upm.edu.my

ABSTRACT

Alzheimer's disease (AD) is a long-lasting brain disorder for which there is no effective treatment. Yet early detection can delay he growth of the disease. Due to the varied nature of medical tests, manual comparison, visualization and analysis of data can be time-consuming as well as demanding. As a result, an effective method for categorization of Magnetic Resonance Imaging (MRI) images is helpful but extremely difficult. In this paper, the stages of AD are identified using a unique method that effectively classifies brain MRI images using label propagation by involving a Deep Learning (DL)-based framework. Decreased brain tissue volume in brain lobes, hippocampus area, and thalamus are the primary features that aid in differentiating an AD from a normal MRI. The features should be efficient in distinguishing the characteristics between an AD-affected brain and a normal one. A Particle swarm optimization (PSO) based Speed-Up Robust Features (SURF) framework that embeds feature vectors in a subspace to maximize utilization of features that were extracted is presented. A classification method is employed in the newly generated space to categorize data into three classes namely, Normal Condition (NC), MCI, and AD using Convolution Neural Network **(**CNN)-MobileNetV2. The proposed scheme offers a classification accuracy is 97% yielding a 3% reduced error rate when compared to the best available approaches.

KEYWORDS: *MCI, AD, CNN, MobileNetV2, PSO, SURF*

1. INTRODUCTION

According to statistics, there are 6.1 million elderly people in India, and about 3.7% of them or 46,000 suffer from Alzheimer's disease (AD). As stated by a Dementia India report, it is anticipated to triple by 2050 as those over 60 are predicted to make up 19.1% of the population. In actuality, there is no efficient method for detecting dementia. The disease's development is slowed down by current treatments. Determining AD at its prodromal stage early on is, therefore crucial[1][2]. A definitive diagnosis can only be made by looking the at patient's brain tissues after the autopsy. There is a definite need for practical advancements in the field of biomarkers for risk assessment, diagnosis, and disease progression tracking [3, 4]. The cost of patient screening is still very high, thus more research is required to create tests that are both affordable and trustworthy. Continued work is still necessary. This includes creating drugs that would impede the progression of AD and other dementia or stop them altogether [5, 6]. Studies are conducted to find new medicines to stop or slow the progression of the disease, as well as biomarkers for diagnosis.

Data mining techniques are used with functional neuroimaging data. Most computer-assisted AD diagnosis techniques currently in use are based on conventional Machine Learning (ML) techniques. The underlying principle of traditional ML

approaches is that the distributions of training, as well as test data, should match. Nevertheless, this assumption is frequently false. This overlooks a substantial share of valuable samples as they have dissimilar but related distributions. Transfer Learning (TL) is recommended to fully utilize labeled samples from comparable distributions. Despite being widely used in numerous fields, few people have employed TL to diagnose AD [7, 8].
MRI images from the Kaggle dataset are used in this study. Within the groups of normal, MCI, and AD, 85 anatomical volumes of interest were investigated. At this step of the investigation, the information gain scales are used. The establishment of a computer model employing TL techniques is the third stage of this research investigation. As a reference source, data from AD and NC are gathered and then compared with MCI images for data classification. The information gain scales are employed in feature optimization to investigate the effects of various characteristics on AD classification [9]. The proposed model uses improved features for ideal classification. The model's application to transfer knowledge to clinical diagnosis is part of the final stages. Figure 1 depicts the difference between Normal MRI and AD affected.

Figure 1Figure 1a: Normal MRI

Figure 1b: AD MRI

2. RELATED WORK

AD detection has been extensively explored and is fraught with problems.An ML-based approach for early AD prediction is proposed by Trambaiolli et al. (2011) [10]. Support Vector Machine (SVM) is used for choosing patterns in EEG signals to detect AD patients from normal cases. To automatically distinguish patients with AD from healthy individuals, a quantitative EEG (qEEG) processing approach is developed in addition to the diagnosis of AD. EEGs from 16 likely mild to moderate symptom AD patients and 19 normal participants are investigated. The accuracy and sensitivity of the EEG epoch analysis are 79.9% and 83.2% respectively. This diagnosis offers accuracy and sensitivity of 87.0% and 91.7% respectively.

Escudero et al (2012) [11] have designed a system for the classification of AD with biomarkers. The customized classifiers reduce the quantity or expense of biomarkers used in the procedure. These classifiers involve fewer but more expensive features, thus improving the classification performance. Additionally, impact of a preliminary analysis of the number of iterations on the evolution of biomarker selection criteria is analysed. Performance declines monotonically from the first to the last rounds.
By using biological and neuroimaging data from the AD Neuroimaging initiative, Gray et al (2013) [12] have proposed a framework with regional MRI volumes, FDG-PET signal intensities based on voxels, CSF biomarker measurements as well as categorical genetic data taken as features. The features of normal patients are compared with the ones suffering from AD and MCI. Classification depending on joint embedding using data from different modalities is better than one involving a single modality.

Sarraf et al (2014) [13] have introduced a system that extracts features for AD/MCI and AD/normal classification by taking high-level latent information from images. To retain intrinsic similarity amid data modalities and data distribution information in every modality, Jie et al (2015) [14] have presented multiple regularised multi-task feature learning schemes Each modality's feature training is referred to as a single

task, and a group-sparsity regularizer is used to capture inherent relatedness amid various modalities as well as jointly choose common features from various tasks.

A novel paradigm for diagnosing AD based on ML and DL techniques is proposed by Mirzaei et al. (2016) [15]. The effectiveness of several ML and DL methods is assessed based on detection accuracy. The testing outcomes show that Bidirectional Long Short-Term Memory (Bi-LSTM) gives a detection accuracy of 91.28%. By analyzing morphological changes of different parts of the brain, Long et al (2017) [16] have suggested an ML-based scheme to classify patients with AD or MCI from healthy ones along with AD conversion in MCI patients. An embedding algorithm for classification is designed with symmetric diffeomorphic registration to compute the distance amid every pair of attributes.

In order to detect AD in its early stages, Asim et al (2018) [17] have used ML algorithms to interpret data collected by neuroimaging technology. Principal Component Analysis (PCA) is employed to minimize the dimensionality of both individual and combined data, and SVMs are employed for classification. Additionally, to assestoficance of specific brain regions i correctly identifying patients, the most frequently prioritized features are used in categorization. The results show that features obtained from numerous atlases perform better than those merely derived from one atlas. Using a single cross-sectional brain structural MRI scan, da Silva et al. (2019) [18] have proposed a DL algorithm to diagnose AD and MIC. CNN is applied on 3D T1-weighted images taken from the Kaggle dataset to classify AD and MCI. HC classification tests offer better accuracy.

Tanveer et al (2020) [19] have used three key ML techniques for diagnosing AD namely, SVM, Artificial Neural Network (ANN), and DL. They have discussed additional learning modalities. This study indicates that SVM-based models demonstrate their reliability. This is due to the fact that SVM does not suffer from local minima problems, unlike approaches like ANN. However, ANNs are more flexible and long-lasting when it comes to incremental learning, modeling data, and quantizing huge dimensional areas. As a result, new ANN variations may one day be applied to AD. Initially, important slices from 3D volumetric data are extracted using maximum Inter-Class Variance (ICV). Then, for every subject, an eigen brain set is created. Third, Welch's t-test is used to determine the most affected eigen brain. Kernel SVM (KSVM) with many kernels is trained using Particle Swarm Optimization (PSO) to forecast AD patients accurately. To identify discriminant areas that separate AD from NC, MIE coefficients with values greater than 0.98 quantiles are considered
.

Liu et al (2020) [20] have employed ML techniques to identify AD using speech data gathered from elderly people that express elements visible in the speech. A fresh speech dataset which includes healthy and is used for experimentation. The DemCare project's speech data is then compared. Logistic regression CV is a tested model that offers the best performance. It is demonstrated that this technique for identifying AD using derived spectrogram characteristics from speech data is efficient. It is proven that the new dataset is reliable and the approaches are proficient.

A plan to investigate ML and novel biomarkers for the identification of AD using a meta-analysis is introduced by Chang et al. (2021) [21]. In addition to AD and tau-related biomarkers, various AD pathology-related biomarkers are used. Neuro Filament Light (NFL) is a neuronal damage biomarker. The ideal prediction model for separating AD patients from healthy ones is built using various ML algorithms. Based on the findings, ML combined with novel biomarkers and a variety of covariates improves the sensitivity and specificity of AD diagnosis. ML algorithms and quick and affordable HPLC for biomarkers help doctors in diagnosing AD in outpatient clinics. Samhan et al (2022) [22] have suggested an approach to predict AD with accurate analysis using ML techniques. The model designed to classify AD is created using Python. The trained model offers 100% accuracy on a set of held-out test images, using 30% of the images for validation and 70% of the image set for training.

3. PRE-PROCESSING OF THE DATASET

MRI neuroimaging samples are taken from Kaggle's Alzheimer's dataset for the proposed work. Skull-stripping and augmentation using image threshold and filtering are common parts of the pre-processing step for brain MRIs. The test image used in this work is pre-processed and enhanced using various filtering techniques.

Segmentation or feature extraction of a noisy image offers poor results. Identification and extraction demand enhancement to obtain better outcomes. Digital Image Processing (DIP) has a wide range of enhancement methods. One of the methods for enhancing images is filtering, which also blurs noise, eliminates high-density noise, and offers density equalization.

3.1 Median Filter (MF)

A non-linear computerized separating technique, median filtering removes noise from an input image or signal. Due to the fact that it preserves edges while eliminating noise in certain circumstances, it is particularly used in the processing of digital images. This technique also has further uses in the field of gesture recognition. The MF calculation adds the input image's median value for pixel estimation. Prior to restoring the calculated pixel with focus point pixel value, pixel points are constructed in mounting order. If the closest picture pixel being considered has an even number of pixels, it replaces that pixel with an average of the values of the two focal point pixels. MF is the most frequently used method due to its capacity to robustly reduce noise with the minimal blurring effect of input noise values with extremely large magnitudes.

3.2 Fast Fourier Transform (FFT)

In order to express the frequency of the gray image, Fast Fourier Transform (FFT) is used, where the high frequency is depicted by the spectrum in the image. Low frequencies are shown in the corners. However, users must have a deep understanding of the system architecture being utilized and must program at a very low level. Since it is difficult to experiment with or create signal/image processing algorithms, they are not helpful. This system details the design and construction of a high-level framework for implementing 1-D and 2-D FFTs for processing MRI images of an AD dataset in an effort to balance the competing demands of increased performance and ease of development. According to the findings, 2-D FFT is implemented in parallel and reaches real-time performance for huge matrices.

FFT computes the Discrete FT (DFT) along with its inverse. It converts digital signal (x) as well as length (N) from the time domain into a signal in the frequency domain (X), as vibration amplitude is recorded based on evolution versus frequency where the signal is found.

$$X[h] = \sum_{i=0}^{N-1}\left(x[i]W_N^{ih}\right), W_N = e^{-\frac{J2\pi}{N}} \quad (1)$$
$$\text{for } h = 0,1,2,\dots,N-1$$

3.3 Discrete Wavelet Transform (DWT)

Wavelet transformations are mathematical operations that separate data into several frequency components with each component taken into account as a resolution scale match. To provide results, the frequency content of MRI is timely examined. The key benefit is the ability to classify signals (Figure 2). Sub-frequency information related to the primary function of the processed signal is used. DWT is given by,

$$W_\varphi(j_0,k) = \frac{1}{\sqrt{M}}\sum_x f(x)\varphi_{j_0,k}(x) \quad (2)$$
$$W_\psi(j,k) = \frac{1}{\sqrt{M}}\sum_k f(x)\psi_{j,k}(x) \quad (3)$$
for $j \geq j_0$

Inerse DWT (IDWT) is given by,

Type equation here.

$$f(x) = \frac{1}{\sqrt{M}}\sum_k W_\varphi(j_0,k)\varphi_{j_0,k}(x) + \frac{1}{\sqrt{M}}\sum_{j=j_0}^{\infty}.\sum_k W_\psi(j,k)\psi_{j,k}(x) \quad (4)$$

where, $f(x)$, $\varphi_{j_0,k}(x)$ and $\psi_{j,k}(x)$ - Discrete functions

Figure 2: Image before (left) and after (right) Filtering

4. FEATURE EXTRACTION

It is the process of picking a subgroup of features to be included while building the model. Diverse signal and image processing scenarios use these feature extraction approaches. A function in the time domain is changed into the frequency domain using FFT and DWT. The image is separated into

blocks, and each block is further broken down into a collection of compact, interconnected areas known as cells. A straightforward one-dimensional centered mask [-1,0,1] is used to calculate the orientate on of the highest gradient and magnitude at each position. The magnitudes are modified for each orientation and cell.

4.1 Histogram Of Oriented Gradients (Hog)

Histograms of directed gradients were offered for human detection. HOG's fundamental principle is that the distribution of gradients of local intensity as well as edge directions frequently effectively defines local object appearance and shape. Object deformations are noticeable to HOG. These distortions are easy for HOG to capture and depict. HOGs are extended to three dimensions to implement directed gradients on 3 orthogonal planes, XY (axial), XZ (coronal), and YZ (sagittal) to define the texture features of pre-processed MRI. This allows the modeling of dynamic textures with HOG.

Algorithm: HOG $(\chi_{t-1}, u_t, z_t, m)$
W_{slow}, W_{fast}
$\bar{\chi}_t = \chi_t = \emptyset$
for $m = 1$ to M do
$X_t^m = \text{motion\_model}(u_t, x_{t-1}^m)$
$W_t^m = \text{measurement\_model}(Z_t, X_t^m, m)$
$\bar{\chi}_t = \bar{\chi}_t + \langle X_t^m, W_t^m \rangle$
$W_{Avg} = W_{Avg} + \frac{1}{M} W_t^m$
End for
$W_{slow} = W_{slow} + \beta_{slow}(W_{avg} - W_{slow})$
$W_{fast} = W_{fast} + \beta_{slow}(W_{avg} - W_{fast})$
for $m = 1$ to M do
with probability $\max\left(0.0, 1.0 - \frac{W_{fast}}{W_{slow}}\right)$
Include arbitrary position to χ_t
Draw $i \epsilon \{1, .., N\}$ with probability $\propto W_t^i$
Add X_t^i to χ_t
End with
End for
return χ_t

4.2 Gray-Level Co-Occurrence Matrix (GLCM)

GLCM creates its value for relevant parts of the image and is used to adapt features from image data and enhance it. There are essentially 11 GLCM features that are shared. Important characteristics for each brain MRI are then extracted for use in categorization, including energy, entropy, homogeneity, contrast, and correlation. The GLCM characteristics are extracted in this phase.

For image with 'p' pixels, 'p × p' co-occurrence matrix (C) on 'n × n' image (I) with an offset$(\Delta x, \Delta y)$ is given by:

$$C_{(\Delta x,\Delta y)}(i,j) = \sum_{x=1}^{n} . \sum_{y=1}^{m} \{1, \text{ if } I(x,y) = i \text{ and } I(x+\Delta x, y+\Delta y) \quad (5)$$

Where,i and j - Pixel values
x and y - Spatial locations in 'I'
$(\Delta x, \Delta y)$ - Offsets that show spatial relation
$I(x + \Delta x, y + \Delta y)$ - Value at pixel (x, y)

4.3 Speeded-Up Robust Features (SURF)

Object recognition in images is accomplished using Speeded Up Robust Features (SURF). of point features, description of point features, and matching of point features. Extraction of point features identifies the pertinent data from a source image. The extracted feature from the image is described in the point feature description. Checking the matched information included in a picture is done via point-feature matching.

4.4 Proposed PSO-based SURF

It is a population-based stochastic search process that mimics the cooperative nature of a flock of birds. It is similar to flocks of migrating birds, where wisdom and effectiveness are derived from the collective effort of the entire flock (Figure 3). The algorithm for the proposed method is given below

Procedure:
Step 1: Import the file and display images
Step 2: Load the input data
Step 3: Convert the training image to RGB
Step 4: Convert the training image to grayscale
Step 5: Generate a test image data with rotational and scale invariant
Step 6: Displays the training and test images.
Step 7: Initialize the parameters of PSO
Step 8: Evaluate the fitness value
Step 9: Calculate the evolutionary factor of each particle
Step10: Update the state in the next generation according to the current state
Step 11: Go to step 7 until the stopping criteria are satisfied.

Journal of Theoretical and Applied Information Technology
15th May 2023. Vol.101. No 9

ISSN: 1992-8645 www.jatit.org E-ISSN: 1817-3195

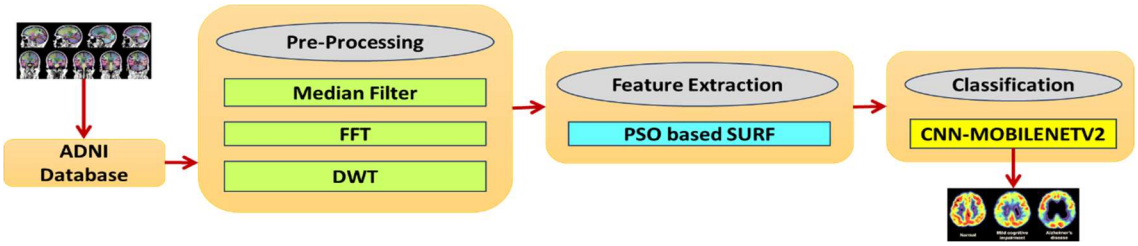

Figure 3: Proposed System Workflow

4. CLASSIFICATION

Classification deals with categorizing data to which a new observation belongs the trained dataset. Convolutional Neural Networks (CNN) is used for classification. CNNs are a subset of DL NNs that are frequently employed in the analysis of visual data and signals. It employs an ANN with a layered structure. In CNN, the network is supplied with distinct features and automatically trained using different datasets. The network educates itself to isolate the disease.

4.1 Convolutional Neural Network (CNN)

CNN is used to develop a classification model as a feature extractor, which means that the architecture, VGG16 pre-trained on ImageNet dataset is used as the basic model using which a brain MRI slice may be passed to determine feature values specific to the MRI slice. As the layer outputs are 1000 class scores for the classification of ImageNet, fully linked base model layers must be deleted in order to use them for our classification challenge.

The final convolutional layer's outcome is flattened into a single column vector after the model's later Fully- Connected (FC) layers are eliminated. New FC layers are added to end of the model, the first of which has 256 neurons, the second is a dropout layer including dropout ratio of 0.5 meaning that half the number of neurons will always output 0, and the last of which is a Softmax layer. When there are more than two classes, Softmax, an activation function that produces a value in the range [0, 1] is frequently utilised.

Procedure:
Input:
l: Input data with true labels
W: Word2 Vec matrix
Output:
Parallel-CNN model on test data
f - featureset 3D matrix
for (i in dataset 'd')
f_i - featureset matrix of sample (i)
for (j in i) do
$V_j = \text{vectorize}(j, w)$
Append V_j to f_i
Append f_i to f
f_{train}, f_{test}, l_{train}, l_{test} = test and trained data for feature set classification and labelling datasets
M=Parallel-CNN (f_{train}, l_{train})
score= evaluate (i, l_{test}, M)
return score

4.2 VGG Very Deep Convolutional Networks (VGGNet)

The Visual Geometry Group (VGG) is a standard deep CNN with many layers. The quantity of layers is called 'deep'. VGG-16 and VGG-19 have 16 and 19 convolutional layers. By using VGG framework, powerful object identification models are constructed. On choosing tasks along with datasets beyond ImageNet, VGGNet designed as Deep NN (DNN) surpasses benchmarks. It is also frequently used for performing image recognition.

VGG-16 Code Implementation steps:

Step 1: Importing Libraries.
Step 1: Importing Libraries.
Step 2: Define input image shape
Step 3: Build a VGG-16 model

4.3 Proposed CNN-MOBILENETV2

The test image serves as the first piece of data followed by pre-processing, which includes converting the test image from RGB to grayscale for processing. The data that is processed is converted into an array for comparison with any pre-existing filters. The second input, the segregated database uses the same preparation method but inculcates the database rather than a picture. Then, CNN is used in training pre-processed data. The trained model and the transformed array are then categorized for making

decisions which makes it clear whether AD is present or not. Figure 3 shows the workflow of the proposed system.

Labeled MRI images are given as input. By using CNN-MobileNetV2, the suggested work demonstrates the early detection of AD. The proposed system includes pre-processing, model extraction, model training and model testing modules to identify AD. The user can choose the input MRI pictures by exploring the drives where the data is stored and waiting to be examined. A linear stack of several NNs makes up MobileNetV2. Flat layer is first produced. The input from the preceding layer is subsequently transformed by the flat layer. The SoftMax activation function is then used to generate a hidden layer with 256 neurons. The dropout layer aids in preventing overfitting. The MobileNetV2 network's convolution is a separable convolution. Convolution kernels and feature combinations are used to filter the features, which creates new representations. Using deep separable convolution, filtering, and additional stages are then combined to create two new steps. The prior stages greatly minimize the cost of computing.

The model consists of eight primary layers in total. CNN learns these feature maps, enabling it to differentiate between the normal stage and AD stage in MR images. Using DL and TL, MobileNetV2 and VGG-16 of CNN models are compared and it is found that the MobileNetV2 model is superior to the VGG-16 model based on accuracy.

Computations are scheduled to reduce the number of tensors which should be stored in memory. It searches through the probable computation orders $\sum G$ and chooses the one which reduces,

$$M(G) = \min_{\pi \epsilon \sum G} \max_{i \epsilon 1 \ldots n} \left[\sum_{A \epsilon R(i,\pi,G)} |A| \text{Size}(\pi_i)\right] \quad (6)$$

Where,

G - Hyper Graph

$R(i, \pi, G)$ - List of intermediary tensors linked to any of $\pi_i \ldots . \pi_n$ nodes

$|A|$ - Size of tensor A

$\text{Size}(\pi_i)$ - Total quantity of memory essential for storage during functioning.

Tensorflow aids in building a Directed Acyclic Compute Hypergraph (G) which includes edges representing operations, and nodes signifying tensors of intermediary computation. For graphs with only insignificant parallel structure, there exists only one non-trivial possible computation order. The total quantity and bound on memory required for inference on 'G' may be simplified:

$$M(G) = \max_{op \epsilon G} \left[\sum_{A \epsilon Op_{inp}} |A| + \sum_{B \epsilon Op_{Out}} |B| + |Op|\right] + \text{Size}(\pi_i) \quad (7)$$

The quantity of memory is the maximum size of inputs as well as outputs across all functions. In case a bottleneck residual block is considered as a single operation, the total memory would be subject to size of bottleneck tensors, instead of tensor size which are internal to bottleneck.

MobileNetV2_CNN

```
def createModel (): #MobileNetV2 model for AD detection
top_model = Sequential()
top_model.add(MobileNetV2(include_top=False, weights="imagenet", input_shape=(224, 224,3)))
top_model.add(Reshape((7,7,1280), input_shape=(-1,7,7,1289)))
top_model.add(Flatten())
top_model.add(Dense(512, activation='relu'))
top_model.add(Dropout(0.5))
top_model.add(Dense(1, activation='sigmoid))
return top_model
model = createModel()
```

5. RESULTS AND DISCUSSION

The system is implemented using Python. MRI samples are taken from Kaggle's Alzheimer' dataset. The data includes 4 classes of images for training as well as testing with 5000 images each. The classes include:

- ✓ Non-Demented
- ✓ Very Mild Demented
- ✓ Mild Demented
- ✓ Moderate Demented

Figure 4 shows the different types of input images and categories of diseases.Images are classified using CNN, VGGNET, MobileNetV2 and CNN MobileNetV2. CNN_ MobileNetV2 offers better classification accuracy (Figure 5).

Figure 6 shows the confusion matrix for classification.

Table 1 shows the PSNR and MSE of feature extract

Journal of Theoretical and Applied Information Technology
15th May 2023. Vol.101. No 9

ISSN: 1992-8645 www.jatit.org E-ISSN: 1817-3195

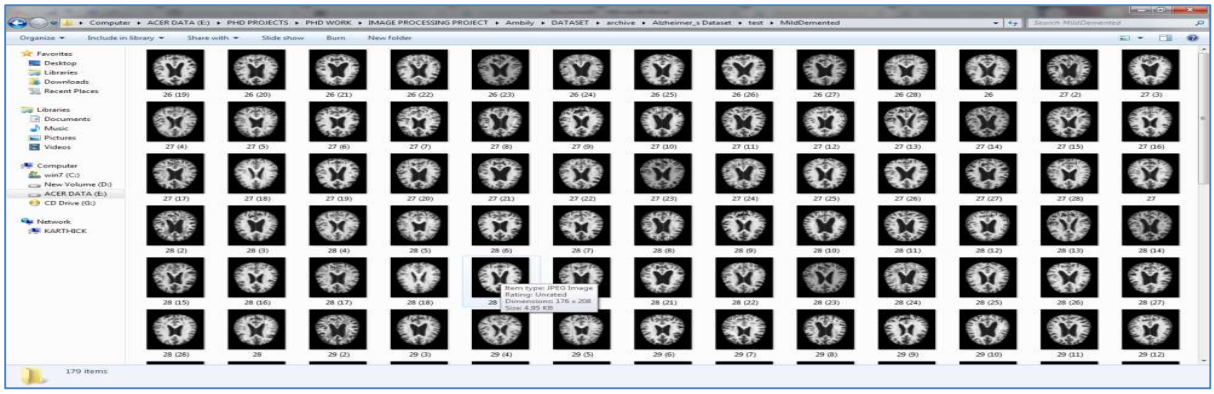

Figure 4: Parameters Analysis

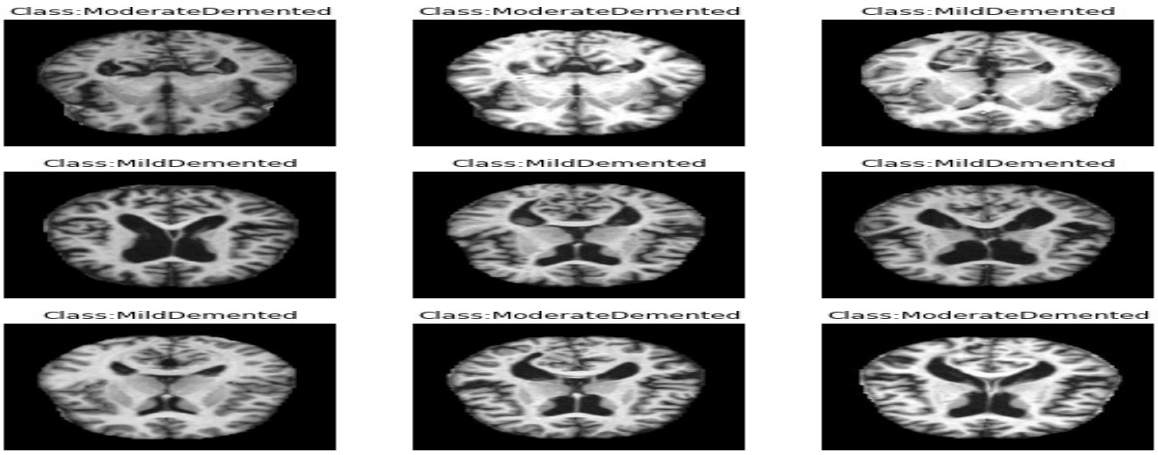

Figure 5: Classification of Images

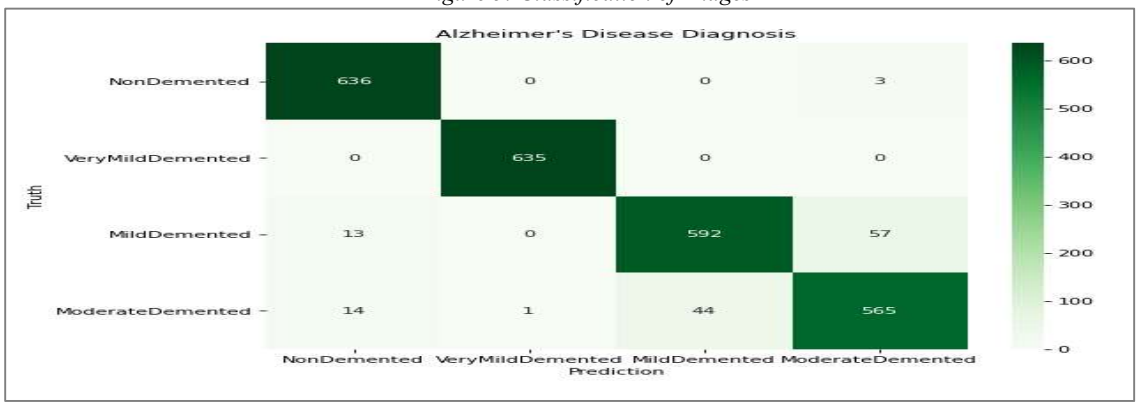

Figure 6: Confusion Matrix of Diseases Classification

Table 1: Feature Extraction

Algorithm	PSNR	MSE
Median	36	0.35
FFT	39	0.28
DWT	43	0.23

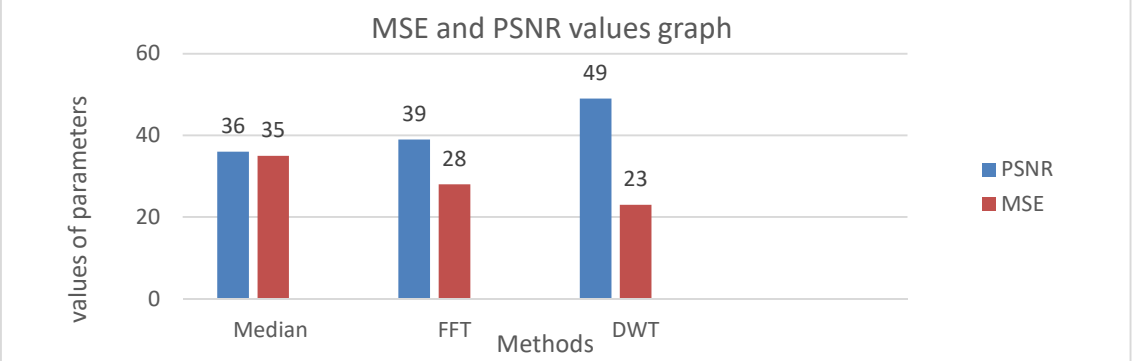

Figure 7 Graphical Representation of MSE and PSNR

.As shown in Figure 7, Median and FFTinvolve 19.4% and 10.3% reduced PSNR respectively and also 52.2% and 21.7% increased MSE respectively when compared to DWT (Table 1).

Table 2: Classification Results

Parameter	Accuracy	Precision	Recall	F-Measure	Time Period
CNN	89	88	89	88	0.56
VGGNET	92	90	92	90	0.48
MobileNetV2	94	92	94	92	0.36
CNN_ MobileNetV2	97	95	97	96	0.31

As shown in Figure 8, CNN, VGGNET, and MobileNetV2 offer 8%, 5%, and 3% lesser Accuracy respectively when compared to CNN_MobileNetV2. Table 2 shows the classification report comparison of accuracy, precision, recall, and f measure for existing methods CNN, VGGNET, Mobilenetv2, and proposed method CNN_Mobilenetv2.

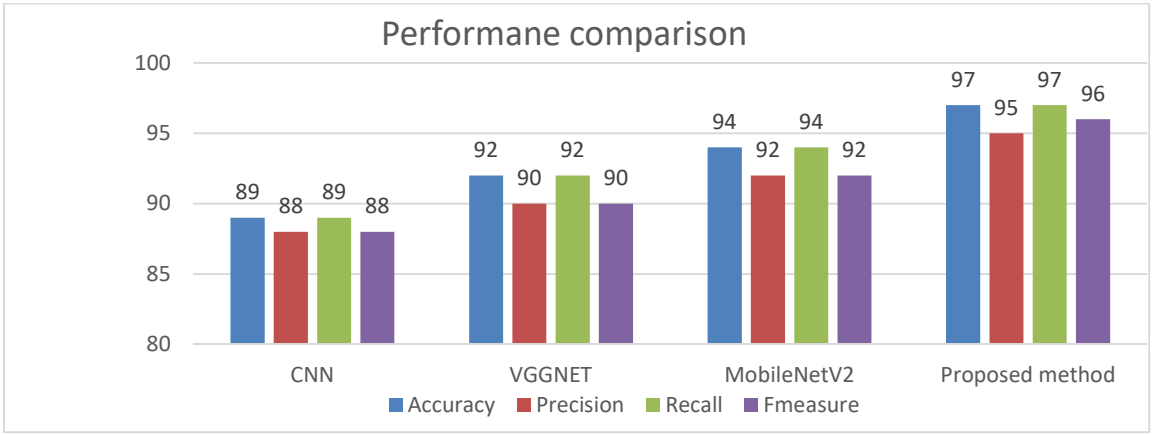

Figure 8: Graphical Representation Of Accuracy, Precision, Recal l,And F Measure.

As shown in Figure 9, CNN, VGGNET and MobileNetV2 involve 61.3%, 48.4% and 32.3% more time respectively when compared to CNN_MobileNetV2.

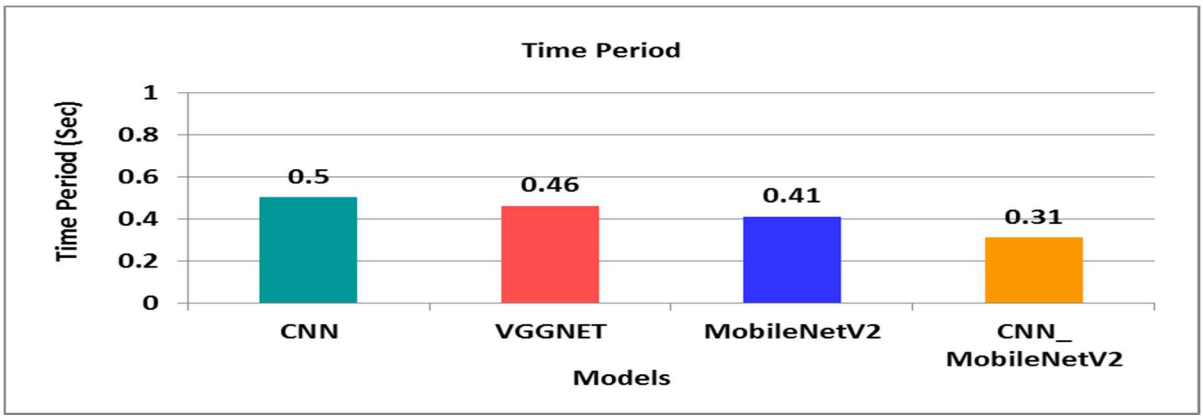

Figure 9: Time period

7. CONCLUSION

It is crucial to identify AD as soon as possible from normal elderly cases. However, the usage of Computer-Aided Diagnosis (CAD) is not widespread, and the performance of the categorization does not meet the benchmark for application in real-world situations. Accurate recognition of both AD patients and their affected brain regions are essential. In this paper, an effective CNN-based MobileNetV2 system is designed to evaluate the severity of brain abnormality caused by AD without using manual procedures which are more difficult to use and prohibitively expensive when providing supportive treatment. Additionally, a thorough analysis of the current feature extraction methods is provided, and PSO-SURF is used to perform feature selection. The conclusion of this investigation supports the notion that the CNN_MobileNetV2 technique provides better classification than benchmarked schemes.

REFERENCES

[1]. Kalló, G., Emri, M., Varga, Z., Ujhelyi, B., Tőzsér, J., Csutak, A., & Csősz, É. (2016). Changes in the chemical barrier composition of tears in Alzheimer's disease reveal potential tear diagnostic biomarkers. PLoS One, 11(6), e0158000.

[2]. Soni, J., Ansari, U., Sharma, D., & Soni, S. (2011). Predictive data mining for medical diagnosis: An overview of heart disease prediction. International Journal of Computer Applications, 17(8), 43-48.

[3]. Williams, J. A., Weakley, A., Cook, D. J., & Schmitter-Edgecombe, M. (2013). Workshops at the twenty-seventh AAAI conference on artificial intelligence.

[4]. Chi, C. L., Oh, W., & Borson, S. (2015, October). Feasibility Study of a Machine Learning Approach to Predict Dementia Progression. In 2015 International Conference on Healthcare Informatics (pp. 450-450). IEEE.

[5]. Chyzhyk, D., & Savio, A. (2010). Feature extraction from structural MRI images based on VBM: data from OASIS database. University of the Basque Country, Internal Research Publication: Basque, Spain.

[6]. Shree, S. B., & Sheshadri, H. S. (2014, December). An initial investigation in the diagnosis of Alzheimer's disease using various classification techniques. In 2014 IEEE International Conference on Computational Intelligence and Computing Research (pp. 1-5). IEEE.

[7]. Patil, T. R. (2013). Sherekar, SS., Performance Analysis of J48 and J48

[8]. Classification Algorithm for Data Classification". International Journal Of Computer Science And Applications, 6(2).

[9]. Ali, J., Khan, R., Ahmad, N., & Maqsood, I. (2012). Random forests and decision trees. International Journal of Computer Science Issues (IJCSI), 9(5), 272.

[10]. Vemuri, P., Gunter, J. L., Senjem, M. L., Whitwell, J. L., Kantarci, K., Knopman, D. S., ... & Jack Jr, C. R. (2008). Alzheimer's disease diagnosis in individual subjects using

structural MR images: validation studies. Neuroimage, 39(3), 1186-1197.
[11]. Trambaiolli, L. R., Lorena, A. C., Fraga, F. J., Kanda, P. A., Anghinah, R., & Nitrini, R. (2011). Improving Alzheimer's disease diagnosis with machine learning techniques. Clinical EEG and neuroscience, 42(3), 160-165.
[12]. Escudero, J., Ifeachor, E., Zajicek, J. P., Green, C., Shearer, J., & Pearson, S. (2012). Machine learning-based method for personalized and cost-effective detection of Alzheimer's disease. IEEE transactions on biomedical engineering, 60(1), 164-168.
[13]. Gray, K. R., Aljabar, P., Heckemann, R. A., Hammers, A., Rueckert, D., & Alzheimer's Disease Neuroimaging Initiative. (2013). Random forest-based similarity measures for multi-modal classification of Alzheimer's disease. NeuroImage, 65, 167-175.
[14]. Sarraf, S., DeSouza, D., Anderson, J., & Tofighi, G. 'DeepAD: Alzheimer's disease classification via deep convolutional neural networks using MRI and fMRI,''bioRxiv, 2016. Google Scholar.
[15]. Jie, B., Zhang, D., Cheng, B., Shen, D., & Alzheimer's Disease Neuroimaging Initiative. (2015). Manifold regularized multitask feature learning for multimodality disease classification. Human brain mapping, 36(2), 489-507.
[16]. Mirzaei, G., Adeli, A., & Adeli, H. (2016). Imaging and machine learning techniques for diagnosis of Alzheimer's disease. Reviews in the Neurosciences, 27(8), 857-870.
[17]. Long, X., Chen, L., Jiang, C., Zhang, L., & Alzheimer's disease Neuroimaging Initiative. (2017). Prediction and classification of Alzheimer disease based on quantification of MRI deformation. PloS one, 12(3), e0173372.
[18]. Asim, Y., Raza, B., Malik, A. K., Rathore, S., Hussain, L., & Iftikhar, M. A. (2018). A multi-modal, multi-atlas-based approach for Alzheimer detection via machine learning. International Journal of Imaging Systems and Technology, 28(2), 113-123.
[19]. da Silva, S. V., Zhang, P., Haberl, M. G., Labrousse, V., Grosjean, N., Blanchet, C., ... & Mulle, C. (2019). Hippocampal mossy fibers synapses in CA3 pyramidal cells are altered at an early stage in a mouse model of Alzheimer's disease. Journal of Neuroscience, 39(21), 4193-4205.
[20]. Tanveer, M., Richhariya, B., Khan, R. U., Rashid, A. H., Khanna, P., Prasad, M., & Lin, C. T. (2020). Machine learning techniques for the diagnosis of Alzheimer's disease: A review. ACM Transactions on Multimedia Computing, Communications, and Applications (TOMM), 16(1s), 1-35.
[21]. Liu, L., Zhao, S., Chen, H., & Wang, A. (2020). A new machine learning method for identifying Alzheimer's disease. Simulation Modelling Practice and Theory, 99, 102023.
[22]. Chang, C. H., Lin, C. H., & Lane, H. Y. (2021). Machine learning and novel biomarkers for the diagnosis of Alzheimer's disease. International Journal of Molecular Sciences, 22(5), 2761.
[23]. Samhan, L. F., Alfarra, A. H., & Abu-Naser, S. S. (2022). Classification of Alzheimer's Disease Using Convolutional Neural Networks. International Journal of Academic Information Systems Research (IJAISR), 6(3).